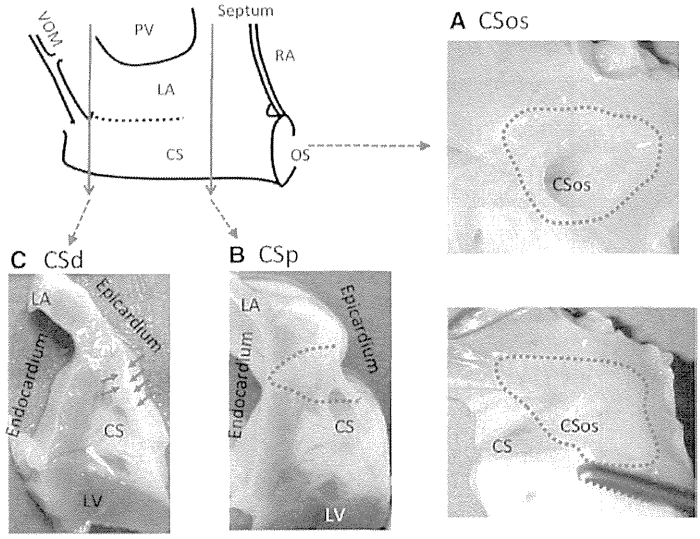

Figure 7. Macroscopic observation of the coronary sinus (CS)–atrial junctions after ablation (ABL). **A**, Ablation lesion around the ostium of CS (CSos). Dotted area showed degeneration by ABL. CS was cut at epicardial ablation site longitudinally in the lower panel. Radiofrequency energy reached within CS. **B**, ABL lesion at the proximal CS (CSp). CS musculature connected to the left atrial (LA) muscles directly at the upper side of the CS. ABL degenerated the CS–LA junctions, LA muscles and upper a-third of the CS musculature. **C**, ABL lesion at the distal CS (CSd). CS was separated from the LA by adipose tissues but small muscular bundle connected the CS and LA (arrows). LV indicates left ventricle; and RA, right atrium.

in whom AF remained after PV isolation.[10] Macroreentrant and focal ATs within the CS have been observed in ≤25% of the patients after PV isolation for AF,[17] and foci within the CS have been reported responsible for 1.4% to 27% of the extra PV foci.[7,9,10,23] Several reports showed the effectiveness of CS-RFCA in eliminating AF after PV isolation,[8–10,24] by

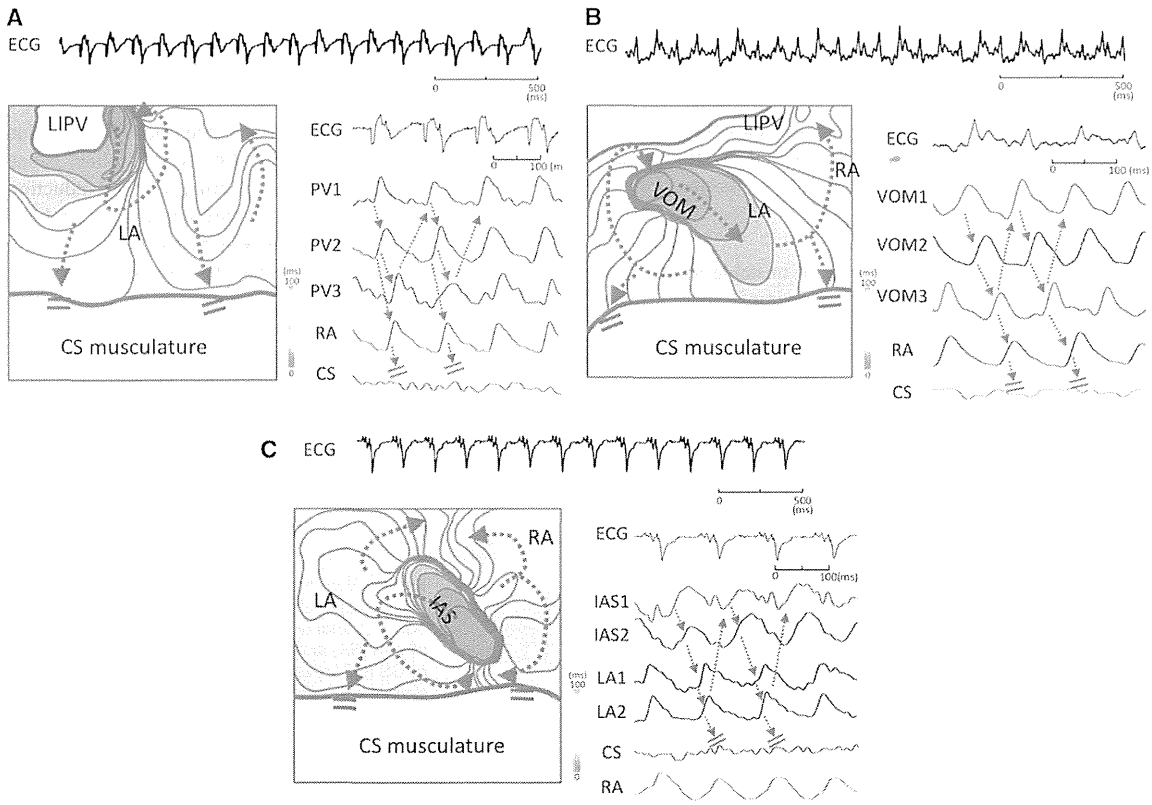

Figure 8. Microreentries after electric isolation of the coronary sinus. **A**, Microreeentry around the left inferior pulmonary vein (LIPV). Counterclockwise reentry was induced by rapid pacing with acetylcholine after the coronary sinus (CS) isolation. **B**, Microreeentry along with the vein of Marshall (VOM). Clockwise reentry was induced by rapid pacing with acetylcholine. **C**, Microreeentry along the intra-atrial septum (IAS). Figure-of-8 reentry was induced by rapid pacing with acetylcholine n. Induced atrial arrhythmias were organized into atrial tachycardia after CS isolation. Note that ECGs represent atrial electrogram and do not include QRS complex. LA indicates left atrium; and RA, right atrium.

disconnecting the LA from the CS musculature[8,9] or by eliminating rapid atrial activity within the CS.[10,24] In long-term AF, complex fractionated atrial electrograms are another target for eliminating AF,[18] and CS is one of the sites where complex fractionated atrial electrograms are frequently recorded after PVs isolation.[18]

Our study supports the mechanism and therapeutic option in patients with AT associated with CS. We induced AT/AF by rapid pacing with or without acetylcholine and showed that the CS musculature can be a part of a macrorentrant circuit and source of microreentry. Acetylcholine abbreviated atrial refractory periods, shortened reentrant circuits, reduced the incidence of macroreentry in the CS and its atrial junctions, and promoted smaller reentrant circuits. The shifting of reentrant circuits and simultaneous existence of multiple reentrant circuits resulted in AF. Microreentry and slow conduction within the CS and functional block at the CS–atrial junctions during AF[2,12–15] can be sources of the rapid electric activity, such as complex fractionated atrial electrograms. Clinically, the importance of PVs on AF initiation and maintenance has been established, so the present model can be applied to instances of recurrent or residual AF after PV isolation.

The CS ablation procedures eliminated micro- and macroreentry associated with the CS musculature and organized the conduction of reentry associated with VOM, interatrial septum and PV.[23] Similar multistep ablation, including PV isolation and linear ablation of the CS, increased the success of AF termination clinically.[24] The microreentry within the CS was less frequent after RFCA in this study, possibly because of the ablation injury in the CS musculature.

Autonomic ganglia are another RFCA target for eliminating AF. Although this model of isolated tissue was separated from the central nervous system, acetylcholine release from local ganglia could still facilitate microreentry during AF. Epicardial RFCA to the CS–atrial junction or VOM would modify autonomic ganglia[25] as well as disconnect the macro- and microreentrant circuits to terminate AF/AF.

Limitations of the Study

We only studied electric activity in the atrial epicardium. Foci and circuits certainly can exist in the endocardium as well,[26] where the activation pattern may be different from what we found in the epicardium.

Application of radiofrequency energy created electric noise in the electrograms so we could not evaluate what step of the ablation procedure terminated AF.

We observed a greater incidence of microreentry in the CS as a driver of acetylcholine-induced AF (88%) than observed clinically. One potential explanation why our AF model differs from clinical AF is that the latter usually occurs after atrial remodeling while we used tissue from healthy canines. In addition, resection of left upper and right PVs in the tissue preparations reduced the electrophysiological substrate of PVs as a role of AF driver.

Conclusions

We showed the efficacy of CS isolation for eliminating AF in the isolated canine atrial model. Rapid pacing induced macroreentrant AF at CS–atrial junctions and microreentry at PV, VOM, and CS. Complete electric isolation of the CS from the atria eliminated reentries associated with the CS and organized AF into AT arising from the PV, intra-atrial septum, and VOM. Additional RFCA to these circuits of the ATs prevented arrhythmias in this model.

Sources of Funding

This research was supported by Krannert Charitable Trust Fund (to D.Z.), Medtronic Japan Fellowship (to H.M.), and American Heart Association, Grant-in-Aid, 455517Z (to J.W.).

Disclosures

None.

References

1. Haïssaguerre M, Jaïs P, Shah DC, Takahashi A, Hocini M, Quiniou G, Garrigue S, Le Mouroux A, Le Métayer P, Clémenty J. Spontaneous initiation of atrial fibrillation by ectopic beats originating in the pulmonary veins. *N Engl J Med.* 1998;339:659–666.
2. Ho SY, Sánchez-Quintana D, Becker AE. A review of the coronary venous system: a road less travelled. *Heart Rhythm.* 2004;1:107–112.
3. Chauvin M, Shah DC, Haïssaguerre M, Marcellin L, Brechenmacher C. The anatomic basis of connections between the coronary sinus musculature and the left atrium in humans. *Circulation.* 2000;101:647–652.
4. Olgin JE, Jayachandran JV, Engesstein E, Groh W, Zipes DP. Atrial macroreentry involving the myocardium of the coronary sinus: a unique mechanism for atypical flutter. *J Cardiovasc Electrophysiol.* 1998;9:1094–1099.
5. Badhwar N, Kalman JM, Sparks PB, Kistler PM, Attari M, Berger M, Lee RJ, Sra J, Scheinman MM. Atrial tachycardia arising from the coronary sinus musculature: electrophysiological characteristics and long-term outcomes of radiofrequency ablation. *J Am Coll Cardiol.* 2005;46:1921–1930.
6. Rotter M, Sanders P, Takahashi Y, Hsu LF, Sacher F, Hocini M, Jaïs P, Haïssaguerre M. Images in cardiovascular medicine. Coronary sinus tachycardia driving atrial fibrillation. *Circulation.* 2004;110:e59–e60.
7. Lin WS, Tai CT, Hsieh MH, Tsai CF, Lin YK, Tsao HM, Huang JL, Yu WC, Yang SP, Ding YA, Chang MS, Chen SA. Catheter ablation of paroxysmal atrial fibrillation initiated by non-pulmonary vein ectopy. *Circulation.* 2003;107:3176–3183.
8. Sanders P, Jaïs P, Hocini M, Haïssaguerre M. Electrical disconnection of the coronary sinus by radiofrequency catheter ablation to isolate a trigger of atrial fibrillation. *J Cardiovasc Electrophysiol.* 2004;15:364–368.
9. Oral H, Ozaydin M, Chugh A, Scharf C, Tada H, Hall B, Cheung P, Pelosi F, Knight BP, Morady F. Role of the coronary sinus in maintenance of atrial fibrillation. *J Cardiovasc Electrophysiol.* 2003;14:1329–1336.
10. Haïssaguerre M, Hocini M, Takahashi Y, O'Neill MD, Pernat A, Sanders P, Jonsson A, Rotter M, Sacher F, Rostock T, Matsuo S, Arantés L, Teng Lim K, Knecht S, Bordachar P, Laborderie J, Jaïs P, Klein G, Clémenty J. Impact of catheter ablation of the coronary sinus on paroxysmal or persistent atrial fibrillation. *J Cardiovasc Electrophysiol.* 2007;18:378–386.
11. Wit A. Coronary sinus electrophysiology and arrhythmogenesis; historical development. In: Chen S, Haissaguerre M, Zipes D, eds. *Thoracic Vein Arrhythmias. Mechanism and Treatment.* Massachusetts: Blackwell; 2004:21–29.
12. Antz M, Otomo K, Arruda M, Scherlag BJ, Pitha J, Tondo C, Lazzara R, Jackman WM. Electrical conduction between the right atrium and the left atrium via the musculature of the coronary sinus. *Circulation.* 1998;98:1790–1795.
13. Kasai A, Anselme F, Saoudi N. Myocardial connections between left atrial myocardium and coronary sinus musculature in man. *J Cardiovasc Electrophysiol.* 2001;12:981–985.
14. Katritsis D, Ioannidis JP, Giazitzoglou E, Korovesis S, Anagnostopoulos CE, Camm AJ. Conduction delay within the coronary sinus in humans: implications for atrial arrhythmias. *J Cardiovasc Electrophysiol.* 2002;13:859–862.
15. Morita H, Zipes DP, Morita ST, Wu J. The role of coronary sinus musculature in the induction of atrial fibrillation. *Heart Rhythm.* 2012;9:581–589. doi:10.1016/j.hrthm.2011.11.041.
16. Tan AY, Chou CC, Zhou S, Nihei M, Hwang C, Peter CT, Fishbein MC, Chen PS. Electrical connections between left superior pulmonary vein, left atrium, and ligament of Marshall: implications for mechanisms of atrial fibrillation. *Am J Physiol Heart Circ Physiol.* 2006;290:H312–H322.

17. Chugh A, Oral H, Good E, Han J, Tamirisa K, Lemola K, Elmouchi D, Tschopp D, Reich S, Igic P, Bogun F, Pelosi F Jr, Morady F. Catheter ablation of atypical atrial flutter and atrial tachycardia within the coronary sinus after left atrial ablation for atrial fibrillation. *J Am Coll Cardiol.* 2005;46:83–91.
18. Arruda M, Natale A. Ablation of permanent AF: adjunctive strategies to pulmonary veins isolation: targeting AF NEST in sinus rhythm and CFAE in AF. *J Interv Card Electrophysiol.* 2008;23:51–57. doi:10.1007/s10840-008-9252-z.
19. Arora R, Verheule S, Scott L, Navarrete A, Katari V, Wilson E, Vaz D, Olgin JE. Arrhythmogenic substrate of the pulmonary veins assessed by high-resolution optical mapping. *Circulation.* 2003;107:1816–1821.
20. Zipes DP, Mihalick MJ, Robbins GT. Effects of selective vagal and stellate ganglion stimulation of atrial refractoriness. *Cardiovasc Res.* 1974;8:647–655.
21. Morita H, Zipes DP, Morita ST, Lopshire JC, Wu J. Epicardial ablation eliminates ventricular arrhythmias in an experimental model of Brugada syndrome. *Heart Rhythm.* 2009;6:665–671. doi:10.1016/j.hrthm.2009.01.007.
22. Kalifa J. Coronary sinus complex fractionated atrial electrograms: when elusive is beautiful. *Heart Rhythm.* 2010;7:1205–1206. doi:10.1016/j.hrthm.2010.06.015.
23. Haïssaguerre M, Hocini M, Sanders P, Takahashi Y, Rotter M, Sacher F, Rostock T, Hsu LF, Jonsson A, O'Neill MD, Bordachar P, Reuter S, Roudaut R, Clémenty J, Jaïs P. Localized sources maintaining atrial fibrillation organized by prior ablation. *Circulation.* 2006;113:616–625.
24. O'Neill MD, Jaïs P, Takahashi Y, Jönsson A, Sacher F, Hocini M, Sanders P, Rostock T, Rotter M, Pernat A, Clémenty J, Haïssaguerre M. The stepwise ablation approach for chronic atrial fibrillation–evidence for a cumulative effect. *J Interv Card Electrophysiol.* 2006;16:153–167.
25. Ulphani JS, Arora R, Cain JH, Villuendas R, Shen S, Gordon D, Inderyas F, Harvey LA, Morris A, Goldberger JJ, Kadish AH. The ligament of Marshall as a parasympathetic conduit. *Am J Physiol Heart Circ Physiol.* 2007;293:H1629–H1635.
26. Katritsis D, Giazitzoglou E, Korovesis S, Paxinos G, Anagnostopoulos CE, Camm AJ. Epicardial foci of atrial arrhythmias apparently originating in the left pulmonary veins. *J Cardiovasc Electrophysiol.* 2002;13:319–323.

CLINICAL PERSPECTIVE

The significant points of this study are (1) the coronary sinus musculature is one of the sources driving atrial fibrillation and (2) isolation of the coronary sinus musculature from the atria converts fibrillatory conduction to organized reentry. Ablation of these residual reentry sites terminated atrial tachycardia/fibrillation. These observations are consistent with the recent demonstration that spiral reentry (rotors) and focal excitation can drive human atrial fibrillation, and catheter ablation of these sources (focal impulse and rotor modulation) can terminate atrial fibrillation and restore sinus rhythm. The reentrant circuits associated with the coronary sinus musculature, Marshall vein, pulmonary veins and atrial septum in this study are probably sources of rotors targeted by focal impulse and rotor modulation in human atrial fibrillation.

Circulation
Arrhythmia and Electrophysiology

American Heart Association.

Isolation of Canine Coronary Sinus Musculature From the Atria by Radiofrequency Catheter Ablation Prevents Induction of Atrial Fibrillation

Hiroshi Morita, Douglas P. Zipes, Shiho T. Morita and Jiashin Wu

Circ Arrhythm Electrophysiol. 2014;7:1181-1188; originally published online November 7, 2014;
doi: 10.1161/CIRCEP.114.001578
Circulation: Arrhythmia and Electrophysiology is published by the American Heart Association, 7272 Greenville Avenue, Dallas, TX 75231

Print ISSN: 1941-3149. Online ISSN: 1941-3084

DOI: 10.1111/echo.12823

Echocardiography

ORIGINAL INVESTIGATION

Left Atrial Appendage Flow Velocity and Time from P-Wave Onset to Tissue Doppler–Derived A′ Predict Atrial Fibrillation Recurrence after Radiofrequency Catheter Ablation

Keiko Fukushima, M.D., Ph.D.,* Noritoshi Fukushima, M.D., Ph.D.,* Koichiro Ejima, M.D., Ph.D.,* Ken Kato, M.D.,* Yasuto Sato, Ph.D.,† Shoko Uematsu, M.D.,* Kotaro Arai, M.D., Ph.D.,* Tetsuyuki Manaka, M.D., Ph.D.,* Atsushi Takagi, M.D., Ph.D.,* Kyomi Ashihara, M.D., Ph.D.,* Morio Shoda, M.D., Ph.D.,* and Nobuhisa Hagiwara, M.D., Ph.D.*

*Department of Cardiology, Tokyo Women's Medical University, Tokyo, Japan; and †Department of Public Health, Tokyo Women's Medical University, Tokyo, Japan

Background: Atrial fibrillation (AF) is associated with atrial remodeling. We investigate the abilities of preprocedural echocardiographic parameters reflecting atrial remodeling to predict AF recurrence after radiofrequency catheter ablation (RFCA) for paroxysmal AF (PAF). Methods: Preprocedural echocardiographic parameters were measured during sinus rhythm in 105 patients with PAF undergoing RFCA. Electrical remodeling was assessed by the time from the onset of the P-wave to the peak A′-wave on the tissue Doppler imaging (PA-TDI), functional remodeling was assessed by the left atrial appendage flow velocity (LAAFV), and structural remodeling was assessed by the left atrial volume index (LAVI). PA-TDI, LAAFV, and LAVI values were divided into tertiles, and their abilities to predict AF recurrence were assessed using Cox regression analysis. Results: AF recurrence occurred in 39/105 (37.1%) patients. After adjustment for confounders, the rate of AF recurrence was significantly higher in the highest tertile of PA-TDI compared with the lowest tertile (≥151.3 msec vs. <131.0 msec; hazard ratio [HR]: 2.477, 95% confidence interval [CI]: 1.031–5.950; P = 0.042), and in the lowest tertile of LAAFV compared with the highest tertile (<48.5 cm/sec vs. ≥64.9 cm/sec; HR: 2.680, 95% CI: 1.136–6.318; P = 0.024). The risk of AF recurrence was also higher in the highest tertile of LAVI (≥34.2 mL/m^2) compared with the lowest tertile, but this difference was not significant (HR: 2.146, 95% CI: 0.834–5.523; P = 0.113). Conclusions: LAAFV (reflecting functional remodeling) and PA-TDI (reflecting electrical remodeling) are independent predictors of AF recurrence after RFCA for PAF. (Echocardiography 2014;00:1–8)

Key words: left atrial appendage flow velocity, total atrial conduction time, left atrial volume index, paroxysmal atrial fibrillation, atrial remodeling, radiofrequency catheter ablation

Atrial fibrillation (AF) induces atrial remodeling, which in turn promotes the continuation of AF,[1,2] and is associated with AF recurrence after radiofrequency catheter ablation (RFCA) for paroxysmal AF (PAF).[3] Atrial remodeling can be distinguished as having electrical, functional, and structural properties. Although molecular mechanisms of these relations have been described in animal models,[4] their relevance is not well characterized in clinical practice. Especially, the relationships between such changes and AF recurrence after RFCA for PAF are not well understood. Left atrial (LA) remodeling can be assessed by echocardiographic parameters, and investigation of the relationships among various preprocedural parameters that reflect LA remodeling may help to predict the risk of AF recurrence in patients who are considering RFCA. Change in the time from the onset of the P-wave to the peak A′-wave on the tissue Doppler imaging (PA-TDI) reflects electrical remodeling,[5,6] change in the LA appendage flow velocity (LAAFV) reflects functional remodeling,[7] and change in the left atrial volume index (LAVI) reflects structural remodeling.[8,9] We previously reported that a longer PA-TDI combined with a higher LAVI on preprocedural echocardiography predicted AF recurrence after RFCA,[10] but this method lacked assessment of functional remodeling. The current study investigated the abilities of the preprocedural PA-TDI, LAVI, and LAAFV values to predict AF recurrence after RFCA for PAF, and analyzed correlations among these three parameters.

Address for correspondence and reprint requests: Keiko Fukushima, M.D., Ph.D., Department of Cardiology, Tokyo Women's Medical University, 8-1 Kawada-cho, Shinjuku-ku, Tokyo 162-8666, Japan. Fax: 81-3-3356-0441;
E-mail: waraugocchin@hotmail.com

Methods:

Study Design and Population:

This study performed a secondary analysis of an existing dataset of 105 consecutive prospectively enrolled patients who underwent RFCA for symptomatic, drug-refractory PAF. The recruitment and data collection methods have previously been described.[10] We previously reported that a combination of PA-TDI and LAVI values could predict AF recurrence, but evaluation of LAAFV was not included in the model. This study investigated the abilities of three echocardiographic parameters that reflect atrial remodeling (PA-TDI, LAAFV, and LAVI) to predict AF recurrence. All patients underwent circumferential pulmonary vein (PV) ablation. PAF was defined as AF that terminated spontaneously within 7 days, according to the HRS/EHRA/ECAS 2007 Consensus Statement on Catheter and Surgical Ablation of AF.[11] Before the procedure, all antiarrhythmic drugs were discontinued for at least five half-lives. Patients who had taken amiodarone were excluded from the study. All patients gave written informed consent.

Echocardiography:

All patients underwent transthoracic echocardiography (TTE) and transesophageal echocardiography (TEE) within 2 days before the scheduled ablation procedure, during sinus rhythm (SR). TTE and TEE were performed using an iE33 ultrasound system (Philips Healthcare, Bothell, WA, USA) with a broadband S4 transducer (2–4 MHz) and an X7-2t TEE transducer. Echocardiography was performed by 2 cardiologists who were blinded to the clinical details and the results. The echocardiographic measurements were performed according to the American Society of Echocardiography guidelines, and the images were stored digitally for playback and analysis. The left ventricular ejection fraction was calculated by the biplane disc method, using apical two- and four-chamber views. The peak velocities of early (E) and late (A) transmitral flow, and early diastolic deceleration time, were measured using pulse Doppler imaging at the level of the mitral leaflet tip in the apical four-chamber view. Early diastolic mitral annular velocity (E′) was recorded in the septal wall of the mitral annulus on tissue Doppler imaging. LA volume was assessed by the biplane disc method, using apical two- and four-chamber views in the end-systolic phase (just before mitral valve opening), and was indexed to body surface area.

Total Atrial Conduction Time:

The PA-TDI duration was used to estimate the total atrial conduction time. The PA-TDI duration has previously been validated as a useful noninvasive method of assessing atrial conduction time.[5] The sample volume was placed on the lateral wall of the mitral annulus in the apical four-chamber view using tissue Doppler imaging. PA-TDI duration was defined as the time from the onset of the P-wave in a surface electrocardiogram to the peak A′-wave of the atrial tissue Doppler tracing. PA-TDI duration was measured in three cardiac cycles and averaged (Fig. 1A). The intraclass correlation coefficient value for intra-observer variability in the PA-TDI duration was 0.816, and the Cronbach's α coefficient for inter-observer variability in the PA-TDI duration was 0.887.

Left Atrial Appendage Flow Velocity:

LAAFV was measured during SR on TEE using pulsed-wave Doppler imaging.[12] The sample volume (4 mm) was positioned 1 cm from the LA appendage orifice in the longitudinal view of the LA appendage.[13] LAAFV was defined as the late diastolic emptying velocity, with the peak of the outflow velocity after the P-wave on an electrocardiogram, and was measured over three cardiac cycles (Fig. 1B).[14]

Electrophysiological Study and Ablation Procedure:

All patients underwent circumferential PV isolation guided by electroanatomical mapping combined with image integration, as described previously.[15] Briefly, a 3.5-mm cooled-tip catheter (Navistar ThermoCool; Biosense Webster Inc., Diamond Bar, CA, USA) was used for mapping and ablation. The circumferential ablation lines were created approximately 2–4 cm from the ipsilateral PV ostia. PV isolation was confirmed by electrograms recorded from two circular mapping catheters, and by pacing maneuvers. After successful circumferential PV isolation, dormant PV conduction was tested by rapid intravenous injection of adenosine triphosphate (20 mg) during an intravenous isoproterenol infusion (5 μg/min), during SR or coronary sinus pacing. If any dormant PV conduction was observed, additional radiofrequency energy was applied to the earliest PV activation site identified by double Lasso catheters at the circumferential ablation lines, until dormant PV conduction was no longer observed.

Postablation Follow-Up:

All patients were hospitalized for 3 days after the ablation procedure, with continuous rhythm monitoring. Class 1 antiarrhythmic drugs were prescribed only if AF recurrence was observed prior to discharge, and were discontinued within 2 months. All patients were scheduled for review at the outpatient clinic at 1, 2, 3, 6, 9, and 12 months after ablation, and then every 6 months. AF recurrence was defined as recurrent symptoms, or documented atrial tachyarrhythmia

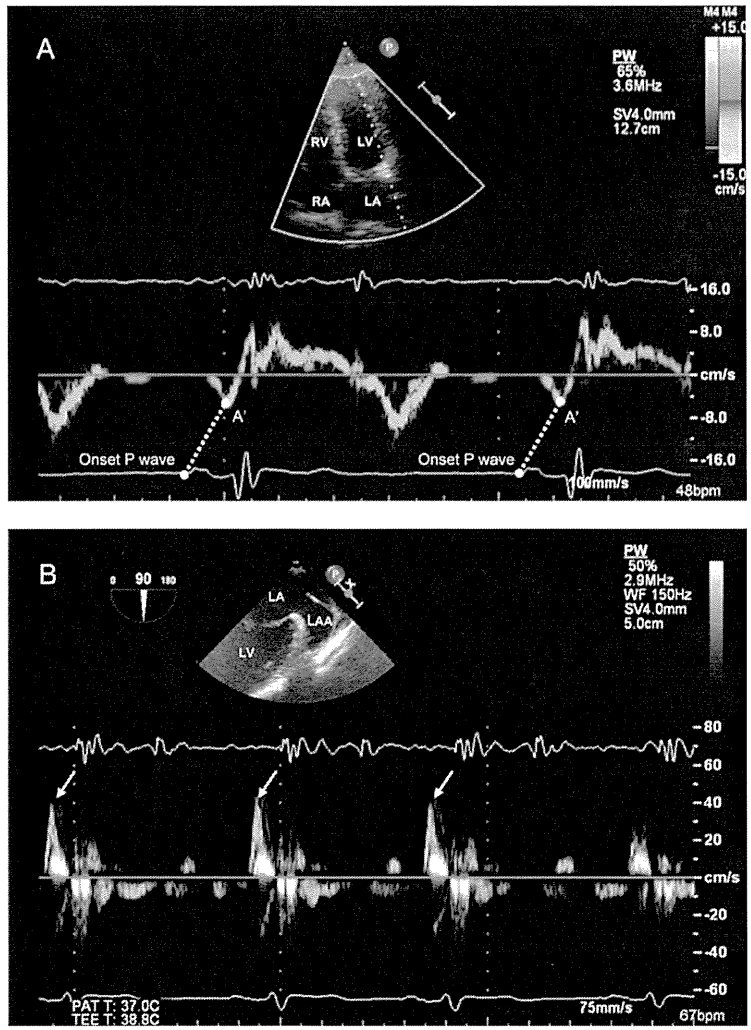

Figure 1. Measurement of time from the onset of the P-wave of the surface electrocardiogram to the peak A′-wave of the atrial tissue Doppler tracing (PA-TDI) duration and LAAFV. **A.** The PA-TDI duration was defined as the time from the onset of the P-wave in lead II of the surface electrocardiogram (ECG) to the peak of the A′-wave of the tissue Doppler velocity curve in the left atrial lateral wall. **B.** LAAFV was defined as the peak outflow velocity after the P-wave on the surface ECG (peak late diastolic emptying velocity, arrows). In the longitudinal view of the LAA, a pulsed-wave Doppler sample was placed 1 cm from the LAA orifice during sinus rhythm. LAAFV = left atrial appendage flow velocity; LAA = left atrial appendage.

(lasting >30 seconds) on electrocardiogram recordings or on 24-hour ambulatory monitoring, at least 2 months after the ablation procedure. Electrocardiography and 24-hour ambulatory monitoring were performed at each follow-up.

Statistical Analysis:
All variables were tested for normality of distribution using the Kolmogorov–Smirnov test. Continuous variables are presented as mean ± standard deviation, or as medians and range, and categorical variables as number and percentage. Comparisons between groups were performed using the Student's unpaired *t*-test or Mann–Whitney *U* test, depending on the distribution of continuous variables. Our previous study found a weak positive correlation between LAVI and PA-TDI,[10] and the current study further analyzed the relationships between LAVI and LAAFV using the Spearman correlation coefficient, and between PA-TDI and LAAFV using the Pearson correlation

coefficient. Categorical variables were compared using the χ^2 test. The PA-TDI, LAAFV, and LAVI values were divided into tertiles based on the distribution of measurements in this study (<33.3rd percentile; 33.3rd–66.6th percentile; >66.6th percentile). The cumulative freedom from AF recurrence was estimated for each tertile of PA-TDI, LAAFV, and LAVI using the Kaplan–Meier method, and tertiles were compared using the log-rank test. Cox regression analysis was used to calculate hazard ratios (HRs) and 95% confidence intervals (CIs), and to perform univariate and multivariate analyses of the associations between the PA-TDI, LAAFV, and LAVI values and AF recurrence. All statistical analyses were performed using IBM SPSS Statistics version 19.0 (IBM, Somers, NY, USA). All tests were two-sided, and $P < 0.05$ was considered to be statistically significant.

Results:

Demographic and Clinical Characteristics:

The baseline characteristics of the patient population are shown in Table I. A total of 105 consecutive patients treated for PAF were included. The mean age of the patients was 57 ± 12 years, and 86 (73.5%) were men. Eleven (10.4%) patients had structural heart disease (five had an atrial septal defect, three had hypertrophic cardiomyopathy, and three had mitral valve prolapse). The median duration of follow-up was 19 months (range 6–38 months). There were no significant differences in age, sex, estimated glomerular filtration rate, brain natriuretic peptide level, serum C-reactive protein level, or the prevalence of hypertension, diabetes mellitus, dyslipidemia, or structural heart disease between patients with and without AF recurrence during the follow-up period.

TABLE I

Baseline Characteristics with or without AF Recurrence after RFCA

	No Recurrence (n = 66)	Recurrence (n = 39)	P
Clinical data			
Age (years)	58 ± 11	57 ± 11	0.578
Male, n (%)	59 (68.6%)	27 (31.4%)	0.260
Body mass index (kg/m^2)	23.6 ± 3.0	24.2 ± 3.4	0.281
Laboratory data			
eGFR (mL/min per 1.73 m^2)	71.6 ± 14.0	72.8 ± 13.7	0.652
CRP (mg/dL)	0.16 ± 0.3	0.12 ± 0.2	0.488
BNP (pg/mL)	44.8 ± 51.9	47.5 ± 41.5	0.778
Comorbidity			
Hypertension, n (%)	35 (53.0%)	15 (38.5%)	0.685
Dyslipidemia, n (%)	24 (36.4%)	12 (30.8%)	0.672
Diabetes mellitus, n (%)	6 (9.0%)	7 (17.9%)	0.225
Structural heart disease, n (%)	5 (7.6%)	6 (15.4%)	0.322

Values are given as mean ± SD, or number (percentage). AF = atrial fibrillation; RFCA = radiofrequency catheter ablation; eGFR = estimated glomerular filtration rate; CRP = serum C-reactive protein; BNP = brain natriuretic peptide.

Echocardiographic Characteristics:

The baseline values of the echocardiographic parameters are shown in Table II. Patients with AF recurrence had a higher LAVI, longer PA-TDI, and lower LAAFV than patients without AF recurrence. There were no significant differences in left ventricular ejection fraction, E/E′, early diastolic deceleration time, or mitral A-wave between patients with and without AF recurrence. The PA-TDI and LAAFV values were normally distributed ($P = 0.200$ and 0.200, respectively) and the LAVI values were not normally distributed ($P = 0.031$). There was a weak negative correlation between LAAFV and LAVI ($r = -0.305$, $P = 0.001$) but there was no significant correlation between LAAFV and PA-TDI ($r = -0.178$, $P = 0.067$).

Relationships between Echocardiographic Parameters that Reflect LA Remodeling and Outcome:

Figure 2 shows Kaplan–Meier curves for freedom from AF recurrence, according to PA-TDI duration

TABLE II

Echocardiographic Parameters in Patients with and without AF Recurrence after RFCA

	No Recurrence	Recurrence	P
LAVI (mL/m^2)	28.1 (12.8–58.9)	33.5 (17.9–78.2)	0.029
E/E′	8.9 ± 3.2	9.6 ± 3.1	0.307
DT (msec)	204.9 ± 52.7	195.6 ± 55.7	0.408
LVEF (%)	55.2 ± 5.3	55.3 ± 6.1	0.943
PA-TDI duration (msec)	137.4 ± 21.5	146.8 ± 21.0	0.030
LAAFV (cm/sec)	59.7 ± 18.9	50.6 ± 19.3	0.019
Mitral A-wave velocity (cm/sec)	62.2 ± 15.2	66.5 ± 29.2	0.334

Results are shown as mean ± SD or median (range). AF = atrial fibrillation; RFCA = radiofrequency catheter ablation; LAVI = left atrial volume index; DT = early diastolic deceleration time; LVEF = left ventricular ejection fraction; PA-TDI = time from the onset of the P-wave of the surface electrocardiogram to the peak A′-wave of the atrial tissue Doppler tracing; LAAFV = left atrial appendage flow velocity.

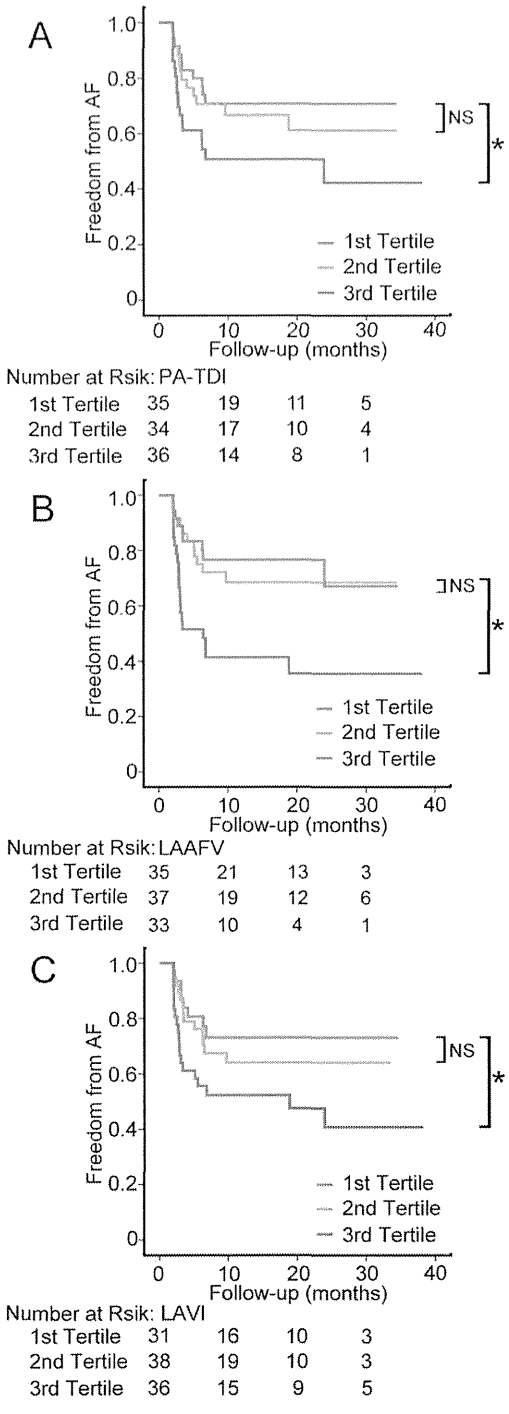

Figure 2. Kaplan–Meier cumulative event-free survival rates for AF recurrence according to tertiles of **A.** PA-TDI, **B.** LAAFV, and **C.** LAVI values. *P < 0.05. NS = not significant; LAVI = left atrial volume index; LAAFV = left atrial appendage flow velocity; AF, atrial fibrillation; PA-TDI = time from the onset of the P-wave of the surface electrocardiogram to the peak A′-wave of the atrial tissue Doppler tracing.

(Fig. 2A), LAAFV (Fig. 2B), and LAVI (Fig. 2C). The tertiles for PA-TDI duration were <131.0, 131.0–151.3, and >151.3 msec; the tertiles for LAAFV were <48.5, 48.5–64.9, and >64.9 cm/sec; and the tertiles for LAVI were <24.2, 24.2–34.2, and >34.2 mL/m^2. AF recurrence was associated with a longer PA-TDI (lowest vs. middle tertile, P = 0.547; lowest vs. highest tertile, P = 0.044; log-rank test; Fig. 2A), lower LAAFV (highest vs. middle tertile, P = 0.791; highest vs. lowest tertile, P = 0.003; log-rank test; Fig. 2B), and higher LAVI (lowest vs. middle tertile, P = 0.483; lowest vs. highest tertile, P = 0.024; log-rank test; Fig. 2C).

Abilities of Factors that Reflect LA Remodeling to Predict AF Recurrence:

AF recurrence occurred in 39 (37.1%) patients during the follow-up period, after the cessation of antiarrhythmic therapy. Cox regression analyses showed a 2.5-fold higher rate of AF recurrence in the highest tertile of PA-TDI duration compared with the lowest tertile (adjusted HR: 2.477, 95% CI: 1.031–5.950; P = 0.042), and a 2.7-fold higher rate of AF recurrence in the lowest tertile of LAAFV compared with the highest tertile (adjusted HR: 2.680, 95% CI: 1.136–6.318; P = 0.024) (Table III). The rate of AF recurrence was also higher in the highest tertile of LAVI compared with the lowest tertile, but this difference was not significant (adjusted HR: 2.146, 95% CI: 0.834–5.523; P = 0.113).

Discussion:

To the best of our knowledge, this is the first study to investigate the abilities of preprocedural PA-TDI (reflecting electrical atrial remodeling), LAAFV (reflecting functional atrial remodeling), and LAVI (reflecting structural atrial remodeling) to predict AF recurrence after RFCA for PAF. Patients with AF recurrence had a higher LAVI, longer PA-TDI, and lower LAAFV than patients without AF recurrence. Longer PA-TDI and lower LAAFV were independent predictors of AF recurrence, with similar predictive values.

AF recurrence is reported to occur in 20–40% of patients at 1–5 years after RFCA.[16] Structural remodeling, including LA enlargement, is a well-known predictor of AF recurrence after RFCA.[17] AF has also been reported to be associated with slow LA conduction, even without detectable structural remodeling.[6,18] Prolonged PA-TDI has previously been reported to be associated with

TABLE III

Predictive Values of Echocardiographic Parameters that Reflect Atrial Remodeling for AF Recurrence after RFCA for Paroxysmal AF

	Unadjusted			Adjusted		
	HR	95% CI	P	HR	95% CI	P
Age (years)	0.996	0.970–1.022	0.739	0.969	0.939–0.999	0.044
Sex (male)	0.705	0.363–1.367	0.300	0.641	0.305–1.349	0.242
LAVI						
Lowest tertile (<24.2 mL/m^2)	Reference			Reference		
Middle tertile (24.2–34.2 mL/m^2)	1.377	0.571–3.324	0.476	1.653	0.631–4.333	0.307
Highest tertile (>34.2 mL/m^2)	2.541	1.111–5.811	0.027	2.146	0.834–5.523	0.113
PA-TDI duration						
Lowest tertile (<131.0 msec)	Reference			Reference		
Middle tertile (131.0–151.3 msec)	1.285	0.555–2.975	0.558	1.873	0.712–4.931	0.204
Highest tertile (>151.3 msec)	2.167	0.999–4.700	0.050	2.477	1.031–5.950	0.042
LAAFV						
Highest tertile (>64.9 cm/sec)	Reference			Reference		
Middle tertile (48.5–64.9 cm/sec)	1.125	0.466–2.714	0.794	1.259	0.501–3.167	0.625
Lowest tertile (<48.5 cm/sec)	3.128	1.420–6.893	0.005	2.680	1.136–6.318	0.024

AF = atrial fibrillation; RFCA = radiofrequency catheter ablation; LAVI = left atrial volume index; DT = early diastolic deceleration time; LVEF = left ventricular ejection fraction; PA-TDI = time from the onset of the P-wave of the surface electrocardiogram to the peak A'-wave of the atrial tissue Doppler tracing; LAAFV = left atrial appendage flow velocity.

an increased risk of new-onset AF[19] and of AF recurrence after cardioversion[20] and RFCA.[21,22] Recently, Kojima et al. reported that poor LA function assessed by velocity vector strain imaging echocardiography was associated with PAF, regardless of LA size.[23] In an animal model, it was found that initial electrical remodeling was associated with changes in cardiac ion channels, and was followed by contractile (functional) remodeling and then structural remodeling.[4] Our results show that PA-TDI duration and LAAFV were independent predictors of AF recurrence, after adjustment for LA dilatation. Together, these findings suggest that slowing of LA conduction and reduction in LA contractile function and may occur in the early stages of LA remodeling in patients with PAF, before structural changes are observed.

This study used LAAFV to assess LA function. However, it is unclear whether LAAFV provides a good reflection of LA function, because of the developmental and structural differences between the LA appendage and the LA main chamber.[24] Agmon et al.[25] found that LAAFV did not provide a good reflection of global LA function. Conversely, Yoshida et al.[26] found a good correlation between LAAFV and LA wall contraction velocity. LAAFV has previously been reported to predict AF recurrence after cardioversion,[27] and Park et al.[28] found that LA appendage mechanical reserve was associated with maintenance of SR after cardioversion. Antonielli et al.[29] also found that a higher LAAFV was associated with better maintenance of SR after cardioversion. Some studies assessed atrial systolic function using mitral inflow and PV flow.[30,31] However, mitral inflow is thought to be affected by age and hemodynamic loading conditions.[32,33] This study found no difference in the mitral inflow A-wave between patients with and without AF recurrence. However, lower LAAFV during SR was an independent predictor of AF recurrence, with a 2.7-fold higher risk of recurrence in the lowest tertile than in the highest tertile.

Preprocedural assessment of the risk of AF recurrence can help to guide patient selection for RFCA. The ability of preprocedural LAAFV to predict AF recurrence therefore has clinical importance in terms of the selection of patients with PAF who are likely to benefit from RFCA. Previous studies also reported an association between LAAFV and thromboembolism in patients with AF.[34,35] Handke et al.[36] reported that LAAFV <55 cm/sec was associated with thrombus formation, independent of heart rhythm. In the current study, LAAFV <48.5 cm/sec was associated with a higher risk of AF recurrence than LAAFV >64.9 cm/sec. Together, these findings suggest that the LAAFV value provides a useful indicator of risk in patients with PAF.

Limitations:

This study has several limitations. First, the rate of AF recurrence may have been underestimated because of undetected asymptomatic AF. Second, the study population was relatively small. Finally, preprocedural atrial stunning after PAF

may have biased the results toward an underestimation of the association between LAAFV and AF recurrence.[37] As this study did not measure changes in LAAFV over time, we could not determine whether recovery of LAAFV from atrial stunning is associated with better clinical outcomes. This potential relationship should be studied in a larger population.

Conclusions:

Preprocedural PA-TDI duration and LAAFV are independent predictors of AF recurrence after RFCA for PAF. Evaluation of functional remodeling by LAAFV and electrical remodeling by PA-TDI may improve risk stratification for AF recurrence after RFCA for PAF.

References

1. Wijffels MC, Kirchhof CJ, Dorland R, et al: Atrial fibrillation begets atrial fibrillation. A study in awake chronically instrumented goats. *Circulation* 1995;92: 1954–1968.
2. Iwasaki YK, Nishida K, Kato T, et al: Atrial fibrillation pathophysiology: Implications for management. *Circulation* 2011;124:2264–2274.
3. Akutsu Y, Kaneko K, Kodama Y, et al: Association between left and right atrial remodeling with atrial fibrillation recurrence after pulmonary vein catheter ablation in patients with paroxysmal atrial fibrillation: A pilot study. *Circ Cardiovasc Imaging* 2011;4:524–531.
4. Allessie M, Ausma J, Schotten U: Electrical, contractile and structural remodeling during atrial fibrillation. *Cardiovasc Res* 2002;54:230–246.
5. Merckx KL, De Vos CB, Palmans A, et al: Atrial activation time determined by transthoracic Doppler tissue imaging can be used as an estimate of the total duration of atrial electrical activation. *J Am Soc Echocardiogr* 2005;18: 940–944.
6. Weijs B, de Vos CB, Limantoro I, et al: The presence of an atrial electromechanical delay in idiopathic atrial fibrillation as determined by tissue Doppler imaging. *Int J Cardiol* 2012;156:121–122.
7. Wang YC, Lin JL, Hwang JJ, et al: Left atrial dysfunction in patients with atrial fibrillation after successful rhythm control for > 3 months. *Chest* 2005;128:2551–2556.
8. Abhayaratna WP, Seward JB, Appleton CP, et al: Left atrial size: Physiologic determinants and clinical applications. *J Am Coll Cardiol* 2006;47:2357–2363.
9. Hoit BD: Left atrial size and function: Role in prognosis. *J Am Coll Cardiol* 2014;63:493–505.
10. Ejima K, Kato K, Arai K, et al: Impact of atrial remodeling on the outcome of radiofrequency catheter ablation of paroxysmal atrial fibrillation. *Circ J* 2014;78: 872–877.
11. European Heart Rhythm Association (EHRA); European Cardiac Arrhythmia Scoiety (ECAS); American College of Cardiology (ACC); American Heart Association (AHA); Society of Thoracic Surgeons (STS), Calkins H, Brugada J, Packer DL, et al: HRS/EHRA/ECAS expert Consensus Statement on catheter and surgical ablation of atrial fibrillation: Recommendations for personnel, policy, procedures and follow-up. A report of the Heart Rhythm Society (HRS) Task Force on catheter and surgical ablation of atrial fibrillation. *Heart Rhythm* 2007;4:816–861.
12. Yao SS, Meisner JS, Factor SM, et al: Assessment of left atrial appendage structure and function by transesophageal echocardiography: A review. *Echocardiography* 1998;15:243–256.
13. Goldberg YH, Gordon SC, Spevack DM, et al: Disparities in emptying velocity within the left atrial appendage. *Eur J Echocardiogr* 2010;11:290–295.
14. Agmon Y, Khandheria BK, Gentile F, et al: Echocardiographic assessment of the left atrial appendage. *J Am Coll Cardiol* 1999;34:1867–1877.
15. Ejima K, Shoda M, Arai K, et al: Impact of diastolic dysfunction on the outcome of catheter ablation in patients with atrial fibrillation. *Int J Caodiol* 2013;164: 88–93.
16. Dewire J, Calkins H: Update on atrial fibrillation catheter ablation technologies and techniques. *Nat Rev Cardiol* 2013;10:599–612.
17. Shin SH, Park MY, Oh WJ, et al: Left atrial volume is a predictor of atrial fibrillation recurrence after catheter ablation. *J Am Soc Echocardiogr* 2008;21:697–702.
18. Teh AW, Kistler PM, Lee G, et al: Electroanatomic remodeling of the left atrium in paroxysmal and persistent atrial fibrillation patients without structural heart disease. *J Cardiovasc Electrophysiol* 2012;23:232–238.
19. De Vos CB, Weijs B, Crijns HJ, et al: Atrial tissue Doppler imaging for prediction of new-onset atrial fibrillation. *Heart* 2009;95:835–840.
20. Maffe S, Paffoni P, Dellavesa P, et al: Prognostic value of total atrial conduction time measured with tissue doppler imaging to predict the maintenance of sinus rhythm after external electrical cardioversion of persistent atrial fibrillation. *Echocardiography* 2014 Jul 22 [Epub ahead of print].
21. den Uijl DW, Gawrysiak M, Tops LF, et al: Prognostic value of total atrial conduction time estimated with tissue Doppler imaging to predict the recurrence of atrial fibrillation after radiofrequency catheter ablation. *Europace* 2011;13:1533–1540.
22. Chao TF, Sung SH, Wang KL, et al: Associations between the atrial electromechanical interval, atrial remodelling and outcome of catheter ablation in paroxysmal atrial fibrillation. *Heart* 2011;97:225–230.
23. Kojima T, Kawasaki M, Tanaka R, et al: Left atrial global and regional function in patients with paroxysmal atrial fibrillation has already been impaired before enlargement of left atrium: Velocity vector imaging echocardiography study. *Eur Heart J Cardiovasc Imaging* 2012;13:227–234.
24. Hara H, Virmani R, Holmes DR, et al: Is the left atrial appendage more than a simple appendage? *Catheter Cardiovasc Interv* 2009;74:234–242.
25. Agmon Y, Khandheria BK, Meissner I, et al: Are left atrial appendage flow velocities adequate surrogates of global left atrial function? A population-based transthoracic and transesophageal echocardiographic study. *J Am Soc Echocardiogr* 2002;15:433–440.
26. Yoshida N, Okamoto M, Beppu S: Validation of transthoracic tissue Doppler assessment of left atrial appendage function. *J Am Soc Echocardiogr* 2007;20:521–526.
27. Palinkas A, Antonielli E, Picano E, et al: Clinical value of left atrial appendage flow velocity for predicting of cardioversion success in patients with non-valvular atrial fibrillation. *Eur Heart J* 2001;22:2201–2208.
28. Park MY, Shin SH, Oh WJ, et al: Prognostic implication of the left atrial appendage mechanical reserve after cardioversion of atrial fibrillation. *Circ J* 2008;72:256–261.
29. Antonielli E, Pizzuti A, Palinkas A, et al: Clinical value of left atrial appendage flow for prediction of long-term sinus rhythm maintenance in patients with nonvalvular atrial fibrillation. *J Am Coll Cardiol* 2002;39:1443–1449.
30. Nakatani S, Garcia MJ, Firstenberg MS, et al: Noninvasive assessment of left atrial maximum dP/dt by a combination of transmitral and pulmonary venous flow. *J Am Coll Cardiol* 1999;34:795–801.

31. Bollmann A: Pulmonary venous flow assessed by Doppler echocardiography in the management of atrial fibrillation. *Echocardiography* 2007;24:430–435.
32. Miyatake K, Okamoto M, Kinoshita N, et al: Augmentation of atrial contribution to left ventricular inflow with aging as assessed by intracardiac Doppler flowmetry. *Am J Cardiol* 1984;53:586–589.
33. Choong CY, Herrmann HC, Weyman AE, et al: Preload dependence of Doppler-derived indexes of left ventricular diastolic function in humans. *J Am Coll Cardiol* 1987;10:800–808.
34. Zabalgoitia M, Halperin JL, Pearce LA, et al: Transesophageal echocardiographic correlates of clinical risk of thromboembolism in nonvalvular atrial fibrillation. Stroke Prevention in Atrial Fibrillation III Investigators. *J Am Coll Cardiol* 1998;31:1622–1626.
35. Kamp O, Verhorst PM, Welling RC, et al: Importance of left atrial appendage flow as a predictor of thromboembolic events in patients with atrial fibrillation. *Eur Heart J* 1999;20:979–985.
36. Handke M, Harloff A, Hetzel A, et al: Left atrial appendage flow velocity as a quantitative surrogate parameter for thromboembolic risk: Determinants and relationship to spontaneous echocontrast and thrombus formation–a transesophageal echocardiographic study in 500 patients with cerebral ischemia. *J Am Soc Echocardiogr* 2005;18:1366–1372.
37. Louie EK, Liu D, Reynertson SI, et al: "Stunning" of the left atrium after spontaneous conversion of atrial fibrillation to sinus rhythm: Demonstration by transesophageal Doppler techniques in a canine model. *J Am Coll Cardiol* 1998;32:2081–2086.

Left ventricular epicardial electrogram recordings in idiopathic ventricular fibrillation with inferior and lateral early repolarization

Koji Nakagawa, MD,* Satoshi Nagase, MD,* Hiroshi Morita, MD,† Hiroshi Ito, MD*

*From the Departments of *Cardiovascular Medicine and †Cardiovascular Therapeutics, Okayama University Graduate School of Medicine, Dentistry, and Pharmaceutical Sciences, Okayama, Japan.*

Introduction

Early repolarization syndrome (ERS) is a primary electrical disease characterized by early repolarization (ER) in the surface ECG and an increased risk of sudden cardiac death because of VF.[1–4]

Experimental studies have suggested that a prominent transient outward current-mediated action potential notch in epicardial cells creates a transmural voltage gradient that results in ER in ERS.[4,5] Ghosh et al[6] studied 2 patients with idiopathic VF and ER by using noninvasive electrocardiographic imaging and demonstrated that their depolarization was normal (homogeneous) but their repolarization was indeed "early" (premature) in some areas that were adjacent to normal repolarizing zones. However, no clinical study has yet been reported that has directly recorded and examined an epicardial electrogram of the LV in patients with ERS.

We observed that patients with Brugada syndrome (BrS) have a prominent potential after the QRS complex and have prolonged repolarization in the epicardium at the right ventricular outflow tract (RVOT), but not in the endocardium.[7,8] Here, we report the first EPS of ERS in which LV epicardial electrogram recording was performed.

Case report

A 42-year-old man had nocturnal cardiac arrest with documented VF and successful resuscitation. He was transferred to a general hospital. ER was indicated in the inferior and lateral leads on the ECG. The results of coronary angiogram, including a vasospasm provocation test, were negative. The patient was transferred to our hospital for the implantation of an implantable cardioverter-defibrillator and confirmation of the diagnosis. The ECG recorded at our hospital also showed ER with J-point elevation of ≥ 0.1 mV above the baseline in the inferior and lateral leads (Figure 1A, left). The results of echocardiography, cardiac catheterization with right and left ventriculography, coronary angiography, and vasospasm provocation test, as well as cardiac magnetic resonance imaging and endomyocardial biopsy were all defined as normal. There was no family history of sudden death. Because no Brugada-type ECG was recorded even after the administration of pilsicainide (Figure 1A, right) and because the QT interval was within the normal range, ERS was confirmed and an implantable cardioverter-defibrillator was implanted.

EPS

After obtaining informed consent, an EPS was performed with local anesthesia. One quadripolar 6-F catheter was introduced from the right femoral vein and positioned at the high right atrium. To record the epicardial electrogram in the LV directly, we introduced a multipolar catheter (Inter Nova Monorail, 8 pole, 2-8-2-8-2 mm interelectrode spacing; Inter Nova Co, Osaka, Japan) from the right femoral vein into the left lateral (marginal) coronary vein, anterior interventricular vein (AIV), and middle cardiac vein (MCV) in a retrograde manner via the coronary sinus (Figure 1B). We recorded local unipolar electrograms with a 0.05- to 100-Hz bandwidth and local bipolar electrograms with a 30- to 100-Hz bandwidth in the LV, respectively. LV epicardial electrograms in the LV were recorded during the sinus rhythm and constant right atrial pacing and after the administration of pilsicainide and isoproterenol. During LV epicardial mapping, pilsicainide, a sodium-channel blocker, was administered at a dose of 1 mg/kg for 5 minutes and isoproterenol was administered at a dose of 1 μg. Unipolar and bipolar endocardial electrograms were also recorded by using a quadripolar 6-F deflectable catheter positioned at the

KEYWORDS Idiopathic ventricular fibrillation; Early repolarization; Early repolarization syndrome; J wave; Epicardium; Left ventricle

ABBREVIATIONS **AIV** = anterior interventricular vein; **BrS** = Brugada syndrome; **ECG** = electrocardiogram; **EPS** = electrophysiological study; **ER** = early repolarization; **ERS** = early repolarization syndrome; **JWS** = J-wave syndrome; **LV** = left ventricle/ventricular; **MCV** = middle cardiac vein; **RVOT** = right ventricular outflow tract; **VF** = ventricular fibrillation

(Heart Rhythm 2014;11:314–317)

Address reprint requests and correspondence: Dr Satoshi Nagase, MD, Department of Cardiovascular Medicine, Okayama University Graduate School of Medicine, Dentistry, and Pharmaceutical Sciences, 2-5-1 Shikata-cho, Kita-ku, Okayama 700-8558, Japan. E-mail address: snagase@cc.okayama-u.ac.jp.

http://dx.doi.org/10.1016/j.hrthm.2013.10.057

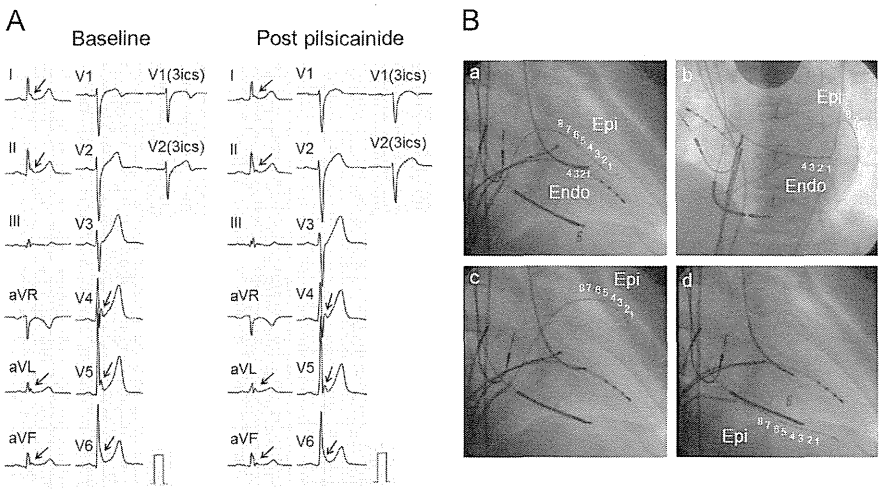

Figure 1 Electrocardiogram and catheter position in the electrophysiological study. **A:** Twelve-lead electrocardiograms at baseline and after pilsicainide administration. Early repolarization (arrows) were recorded in the inferior and lateral leads both at baseline and after pilsicainide administration. 3ics = third intercostal space. **B:** Catheter position in the electrophysiological study. The multipolar catheter was introduced into the lateral coronary vein (**a** and **b**), anterior interventricular vein (**c**), and middle cardiac vein (**d**), as well as the quadripolar catheter at the endocardium in the left ventricular opposite the epicardial mapping site of the lateral coronary vein (**a** and **b**). Panels **a**, **c**, and **d** are right anterior oblique view, and panel **b** is left anterior oblique view. Epi = epicardial; Endo = endocardial.

endocardium in the LV opposite the epicardial mapping site of the lateral coronary vein.

Prominent J waves were observed on unipolar recording, and potentials were observed after the QRS complex on bipolar recording at the epicardium of the LV from the left lateral vein (Figures 2A and 2B). The J wave observed on unipolar recording almost coincided with the potential after the QRS complex observed with bipolar recording and also

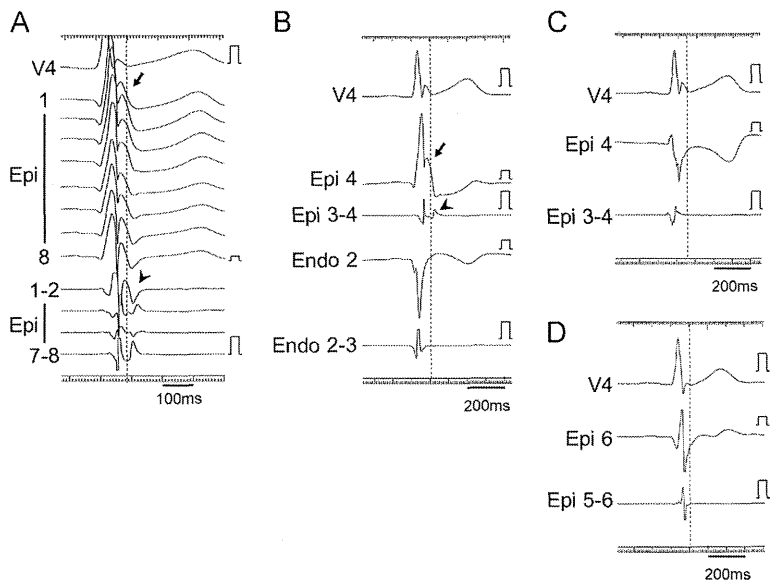

Figure 2 Electrograms at the epicardium (Epi) and endocardium (Endo) in the electrophysiological study. **A:** Unipolar (Epi 1 to 8) and bipolar (Epi 1-2 to 7-8) electrograms at the lateral coronary vein of the left ventricular (LV) epicardium. Prominent J waves (arrow) were observed on unipolar recording, and potentials (arrow head) were observed after the QRS complex on bipolar recording from all leads in the left lateral coronary vein. The J wave with unipolar recording almost coincided with the potential after the QRS complex with bipolar recording and also coincided with early repolarization in the electrocardiogram (lead V_4). **B:** Unipolar (Epi 4, Endo 2) and bipolar (Epi 3-4, Endo 2-3) electrograms at the lateral coronary vein of the LV epicardium and at the opposite area within the endocardium. The prominent J wave (arrow) and the potential after the QRS complex (arrow head) were observed from the left lateral coronary vein. The J wave and the potential after the QRS complex were not recorded within the endocardium at the opposite area. **C:** Unipolar (Epi 4) and bipolar (Epi 3-4) electrograms recorded at the anterior interventricular vein of the LV epicardium. The J wave and the potential after the QRS complex were not recorded at the anterior interventricular vein. **D:** Unipolar (Epi 6) and bipolar (Epi 5-6) electrograms recorded at the middle cardiac vein of the LV epicardium. The J wave and the potential after the QRS complex were not recorded at the middle cardiac vein.

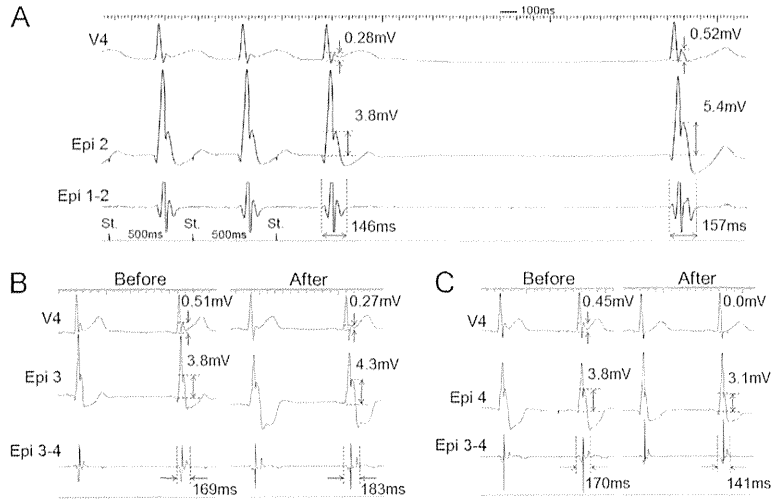

Figure 3 Epicardial electrogram (Epi) at the lateral coronary vein in the electrophysiological study. **A:** Unipolar (Epi 2) and bipolar (Epi 1-2) electrograms during and just after constant atrial pacing (cycle length = 500 ms). The J wave with unipolar recording was diminished, and the duration of the potential with bipolar recording was shortened during constant atrial pacing. Early repolarization (ER) in lead V_4 was also slightly diminished with constant atrial pacing. Pause-dependent augmentations of the J wave in the epicardium and ER in lead V_4 were also observed. **B:** Unipolar (Epi 3) and bipolar (Epi 3-4) electrograms before and after pilsicainide administration. The J wave with unipolar recording was accentuated, and the duration of the potential with bipolar recording was prolonged by pilsicainide administration. ER was slightly diminished; however, S wave also appeared in lead V_4 after pilsicainide administration. **C:** Unipolar (Epi 4) and bipolar (Epi 3-4) electrograms before and after isoproterenol administration. The J wave with unipolar recording was diminished, and the duration of the potential with bipolar recording was shortened by isoproterenol administration. ER in lead V_4 was also diminished.

almost coincided with ER observed on the ECG. The J wave and the potential after the QRS complex were not recorded within the endocardium at the opposite area (Figure 2B). Both the J wave observed on unipolar recording and the potential recorded on bipolar recording at the LV epicardium were diminished on constant atrial pacing (Figure 3A). The J wave on unipolar recording and the potential on bipolar recording at the LV epicardium were accentuated after pilsicainide administration but were diminished after isoproterenol administration (Figures 3B and 3C). VF was not induced with triple extrastimulation performed from the right ventricular apex, RVOT, and LV endocardium but was induced from the LV epicardium by using the catheter in the left lateral vein at twice diastolic threshold (S1S1: 400 ms; S1S2: 220 ms; S2S3: 210 ms; S3S4: 210 ms). Neither J waves on unipolar recording nor potentials after the QRS complex on bipolar recording were detected at the AIV or MCV (Figures 2C and 2D).

Discussion

We previously reported delayed electrograms at the RVOT epicardium in BrS.[7] Nademanee et al[9] also reported that the delayed bipolar electrogram at the RVOT epicardium coincided with the unipolar J-point elevation, which is identical to the typical Brugada-type ECG. The result of their report is quite similar to the finding in our case. We could find delayed bipolar electrogram and unipolar J-point elevation at the epicardium of the lateral LV in idiopathic VF with ER. Bipolar delayed potential almost coincided with unipolar J-point elevation, which was similar to inferior and lateral ER in the ECG.

J wave and delayed potential

Antzelevitch and Yan[5] proposed that ERS was one form of J-wave syndrome (JWS) and that JWS was associated with prominent, transient, outward current-mediated action potential notches in epicardial cells. The cause of the J wave in JWS and its correlation with VF remain unresolved in our study. However, EPS findings suggest that the J wave in the LV epicardium could be associated with a repolarization feature because the J wave diminished on constant atrial pacing and isoproterenol administration.[10] Pause-dependent augmentations of the J wave in the epicardium and the ER on the ECG were also observed. The significance of pause-dependent augmentation of ER of the ECG in idiopathic VF was already reported.[1,11,12] The characteristics of the J wave in the LV epicardium were similar to those of the transient outward current–mediated action potential notch. Because the J wave with unipolar recording coincided with the bipolar potential after the QRS complex and because the responses to constant atrial pacing and administration of pilsicainide and isoproterenol are similar, the J wave with unipolar recording might be associated with delayed bipolar potential. The potential after the QRS complex that was observed on bipolar recording in the LV epicardium in this case is similar to the post-QRS potential observed in BrS, as reported by Aizawa et al.[13]

Epicardial J wave and ER on the ECG

The responses to constant atrial pacing and isoproterenol administration are similar between the J wave in the LV epicardium and ER on the ECG. The administration of pilsicainide exacerbates epicardial J waves; however, ER did not show this tendency on the ECG. We assume that the

administration of pilsicainide may augment local epicardial J waves in the LV. However, pilsicainide administration also causes conduction delay in the entire heart and affects the configuration of the QRS and also the ER. In fact, prominent S wave appeared in lead V_4 after pilsicainide administration (Figures 1A and 3B). There is a possibility that the conduction delay of the far-field myocardium and a minor axis deviation could mask the change of the local epicardial J wave in the LV. Similarly, the administration of a sodium-channel blocker augments ST-segment elevation in the right precordial leads in BrS and augments epicardial J wave in the lateral LV in ERS.

Location of the arrhythmic substrate

Because prominent epicardial J waves were recorded only at the LV epicardium from the left lateral coronary vein but not from the AIV, MCV, or LV endocardium and because VF was induced with the programmed stimulation at the LV epicardium but not at the RVA, RVOT, or LV endocardium, we speculate that the LV epicardial myocardium may be associated with an arrhythmogenic substrate in this patient with idiopathic VF.

Study limitations

The main limitation of our study is the explanation of the downslope of the excitation component of the unipolar electrogram which we called epicardial J wave. We assume that because the ECG especially in the precordial lead is the unipolar recording from the body surface with a 0.05- to 100-Hz bandwidth, LV epicardial electrogram with the same unipolar recording and the same bandwidth could show similar and more accurate information about "ER" (J wave). In fact, the morphology of the ECG in left precordial lead was similar to that of the LV epicardial electrogram. It is still controversial whether the "ER" (J wave) of the surface ECG and epicardial J wave in JWS with a history of VF represents the abnormality of repolarization or depolarization. However, the downslope of the component of the LV unipolar electrogram (J wave) might represent the J wave in the ECG.

Another main limitation is that we were able to record electrograms only at the site through which the major epicardial vein in the LV runs. We could not, therefore, perform detailed mapping in the LV epicardium. In addition, this is only a case report. Thus, our results should be confirmed by studies of consecutive patients with malignant ER (ER with a history of VF), of healthy individuals with apparently benign ER, and of healthy individuals without ER.

Conclusion

We report the first case of idiopathic VF with inferior and lateral ER in which LV epicardial electrogram recording was performed. In EPS, we recorded prominent J waves and potentials after the QRS complex at the epicardium of lateral LV, but not within the endocardium at the opposite area. These features were accentuated on pilsicainide administration but diminished on constant atrial pacing and isoproterenol administration. The epicardial J wave coincided with the ER on ECG. Atrial pacing and isoproterenol diminished ER, however, pilsicainide also diminished ER with accentuated S wave in lead V4. This might be due to the transmural or far-field conduction delay causing the J wave to merge with the S wave. VF was induced with programmed stimulation only from lateral LV epicardium. The epicardial myocardium of the LV might contribute to arrhythmogenesis in this patient.

References

1. Aizawa Y, Tamura M, Chinushi M, et al. Idiopathic ventricular fibrillation and bradycardia-dependent intraventricular block. Am Heart J 1993;126:1473–1474.
2. Haissaguerre M, Derval N, Sacher F, et al. Sudden cardiac arrest associated with early repolarization. N Engl J Med 2008;358:2016–2023.
3. Rosso R, Kogan E, Belhassen B, et al. J-point elevation in survivors of primary ventricular fibrillation and matched control subjects: incidence and clinical significance. J Am Coll Cardiol 2008;52:1231–1238.
4. Nam GB, Kim YH, Antzelevitch C. Augmentation of J waves and electrical storms in patients with early repolarization. N Engl J Med 2008;358:2078–2079.
5. Antzelevitch C, Yan GX. J wave syndromes. Heart Rhythm 2010;7:549–558.
6. Ghosh S, Cooper DH, Vijayakumar R, et al. Early repolarization associated with sudden death: insights from noninvasive electrocardiographic imaging. Heart Rhythm 2010;7:534–537.
7. Nagase S, Kusano KF, Morita H, et al. Epicardial electrogram of the right ventricular outflow tract in patients with the Brugada syndrome: using the epicardial lead. J Am Coll Cardiol 2002;39:1992–1995.
8. Nagase S, Kusano KF, Morita H, et al. Longer repolarization in the epicardium at the right ventricular outflow tract causes type 1 electrocardiogram in patients with Brugada syndrome. J Am Coll Cardiol 2008;51:1154–1161.
9. Nademanee K, Veerakul G, Chandanamattha P, et al. Prevention of ventricular fibrillation episodes in Brugada syndrome by catheter ablation over the anterior right ventricular outflow tract epicardium. Circulation 2011;123:1270–1279.
10. Antzelevitch C. Late potentials and the Brugada syndrome. J Am Coll Cardiol 2002;39:1996–1999.
11. Aizawa Y, Sato A, Watanabe H, et al. Dynamicity of the J-wave in idiopathic ventricular fibrillation with a special reference to pause-dependent augmentation of the J-wave. J Am Coll Cardiol 2012;59:1948–1953.
12. Haissaguerre M, Sacher F, Nogami A, et al. Characteristics of recurrent ventricular fibrillation associated with inferolateral early repolarization role of drug therapy. J Am Coll Cardiol 2009;53:612–619.
13. Aizawa Y, Chinushi M, Tagawa M, et al. A post-QRS potential in Brugada syndrome: its relation to electrocardiographic pattern and possible genesis. J Am Coll Cardiol 2008;51:1720–1721.

Europace (2014) **16**, 1828–1837
doi:10.1093/europace/euu063

Long QT syndrome type 8: novel *CACNA1C* mutations causing QT prolongation and variant phenotypes

Megumi Fukuyama[1], Qi Wang[1], Koichi Kato[1], Seiko Ohno[1,2], Wei-Guang Ding[3], Futoshi Toyoda[3], Hideki Itoh[1], Hiromi Kimura[1], Takeru Makiyama[2], Makoto Ito[1], Hiroshi Matsuura[3], and Minoru Horie[1]*

[1]Department of Cardiovascular and Respiratory Medicine, Shiga University of Medical Science, Seta-Tsukinowa, Otsu, Shiga 520-2192, Japan; [2]Department of Cardiovascular Medicine, Kyoto University Graduate School of Medicine, Kyoto 606-8507, Japan; and [3]Department of Physiology, Shiga University of Medical Science, Shiga 520-2192, Japan

Received 14 January 2014; accepted after revision 5 March 2014; online publish-ahead-of-print 12 April 2014

Aims *CACNA1C* mutations have been reported to cause LQTS type 8 (LQT8; Timothy syndrome), which exhibits severe phenotypes, although the frequency of patients with LQT8 exhibiting only QT prolongation is unknown. This study aimed to elucidate the frequency of *CACNA1C* mutations in patients with long QT syndrome (LQTS), except those with Timothy syndrome and investigate phenotypic variants.

Methods and results *CACNA1C* gene screening was performed in 278 probands negative for LQTS-related gene mutations. Functional analysis of mutant channels using a whole-cell patch-clamp technique was also performed. Using genetic screening, we identified five novel *CACNA1C* mutations: P381S, M456I, A582D, R858H, and G1783C in seven (2.5%) unrelated probands. Seven mutation carriers showed alternative clinical phenotypes. Biophysical assay of *CACNA1C* mutations revealed that the peak calcium currents were significantly larger in R858H mutant channels than those of wild-type (WT). In contrast, A582D mutant channels displayed significantly slower inactivation compared with WT. The two mutant channels exerted different gain-of-function effects on calcium currents.

Conclusion In patients with LQTS, the frequency of *CACNA1C* mutations was higher than reported. Even without typical phenotypes of Timothy syndrome, *CACNA1C* mutations may cause QT prolongation and/or fatal arrhythmia attacks.

Keywords Long QT syndrome • L-type calcium channels • L-type calcium current • Genetics • Arrhythmia

Introduction

Long QT syndrome (LQTS) is a primary cardiac channelopathy generally characterized by a prolongation of the corrected QT (QTc) interval, syncope, ventricular arrhythmias, and high risk of sudden cardiac death.[1] Its prevalence has recently been estimated at ~1 : 2000.[2] This disease is genetically heterogeneous, and 15 genes are responsible for LQTS.[3]

$Ca_V1.2$ protein encoded by *CACNA1C* gene is α_1-subunits of cardiac L-type calcium channel (LTCC) and constitutes the ion permeating subunit, which determines the main biophysical and pharmacological properties of the channel.[4]

In 2004, a *CACNA1C* mutation (G406R) was identified in patients with Timothy syndrome or LQTS type 8 (LQT8), a specific subtype of LQTS.[5] The syndrome has been considered to be a rare variant of LQTS, accompanied by severe phenotypes and early fatality. Its extracardiac phenotypes involve multiple organ systems and include congenital heart disease, syndactyly, immune deficiency, and central nervous system and metabolic abnormalities, justifying its separate classification. Since the first report, only two *CACNA1C* mutations have been reported in patients with LQT8: p.G402S and p.G406R.[6]

In autosomal dominant inherited LQTS, without any clinical signs suggestive of Timothy syndrome,[7] three *CACNA1C* mutations were identified by whole-exome sequencing. Accordingly, the number of variations of *CACNA1C* mutations remains small. On the other hand, in our previous study,[8] we identified LTCC-related genes in seven probands with Brugada syndrome and idiopathic ventricular

* Corresponding author. Tel: +81 77 548 2213; fax: +81 77 543 5839. *E-mail address*: horie@belle.shiga-med.ac.jp

What's new?

- In this study, five novel variants in *CACNA1C* were identified, presenting the long QT syndrome (LQTS) without Timothy syndrome phenotype. This study reports variations of *CACNA1C* mutations in LQT8 about their topological locations, clinical phenotypes, and functional changes.
- In the functional analysis, two mutations were found to significantly increase the I_{Ca} current density.
- The frequency of *CACNA1C* mutation in LQTS was suspected to be higher than that previously reported, and the severity oftheir phenotype was more than reported for Timothy syndrome.

fibrillation (VF). We therefore raised a possibility that *CACNA1C* variants were associated with other types of fatal arrhythmic diseases including LQTS. In our cohort, there are many LQTS probands in whom no causative gene has been identified. This study aims to identify *CACNA1C* mutation carriers among LQTS probands using direct sequencing to investigate the variant of clinical phenotypes and effects of mutant channels on phenotype and functional analysis.

Patient cohort and methods

Subjects

The study cohort included 278 Japanese probands registered at the Shiga University of Medical Science and Kyoto University Graduate School of Medicine between 1996 and 2012 for genetic analysis. They were suspected as clear or potential [whose electrocardiography (ECG) showed borderline QT prolongation] LQTS, showing one or more of the following phenotypes: QT prolongation in 12-lead ECG or personal/family history of syncope, seizures, sudden death, severe bradycardia for their age,[9] or arrhythmic events. QT intervals were manually measured in lead II or V5, as shown on 12-lead ECG.[2] QT intervals were corrected (QTc) for the heart rate (HR) using Bazett's formula. In brief, the ECG criteria for QTc intervals are ≥440 ms for males and ≥460 ms for females.[10] The LQTS risk score (Schwartz score) was calculated following 1993–2012 LQTS diagnostic criteria.[3] In the recent consensus for LQTS diagnosis,[11] the cut-off value of Schwartz score is ≥3.5 points; however, not all patients in our cohort fulfilled the diagnostic requirements. In our cohort, 123 of 278 (44%) had ≥3.5 points on the score. Because patients with cardiomyopathy were excluded, their ejection fractions were not reduced in echocardiograms. All subjects gave written informed consent in accordance with the guidelines approved by each institutional review board.

Gene scanning

Genomic DNA was extracted from peripheral blood leucocytes. Gene screening was performed using high-resolution melting (HRM)[12] or denaturing high-performance liquid chromatography (dHPLC; WAVE system Model 3500; Transgenomic) and subsequent direct sequencing, as previously reported.[8] To detect any homozygous mutations, we mixed the samples from two unrelated probands on HRM and dHPLC screening. The probands were negative for mutations and single nucleotide polymorphisms (SNPs), which were reported to affect the QT prolongation in *KCNQ1*, *KCNH2*, *SCN5A*, *KCNE1*, *KCNE2*, and *KCNJ2*. According to previous reports,[13,14] the possible impact of amino acid substitutions on the structure and function of human protein was evaluated using three prediction software packages, PolyPhen-2 (http://genetics.bwh.harvard.edu/pph2/), MutPred (http://mutpred.mutdb.org/), and Align GVGD (http://agvgd.iarc.fr/agvgd_input.php).

Mutagenesis and functional expression

The human wild-type (WT) *CACNA1C* cDNA tagged by (EYFP) $N\alpha_{1c,77}$ in pcDNA vector and cDNAs of *CACNB2b* and *CACNA2D1*, both cloned in pcDNA3.1 vector (Invitrogen), were used. Vectors were gifts from Dr Charles Antzelevitch (Masonic Medical Research Laboratory). Site-directed mutagenesis was performed using QuickChange-II-XL kit (Stratagene). Mutated genes were functionally expressed in Chinese hamster ovary (CHO) cells. Chinese hamster ovary cells were transfected with cDNA encoding WT or mutant *CACNA1C* subunits (2 μg) along with cDNA encoding *CACNB2b* (0.5 μg) and *CACNA2D1* (0.5 μg) using 6 μL of Fugene 6 (Roche Diagnostics).[5] Chinese hamster ovary cells were perfused with an external solution containing the following (in mmol/L): N-methyl-d-glucamine, 130; KCl, 5; $CaCl_2$, 15; $MgCl_2$, 1; and 4-(2-hydroxyethyl)-1-piperazineethanesulfonic acid (HEPES), 10 (pH 7.35 with HCl). Recording pipettes were filled with an internal solution containing the following (in mmol/L): $CsCl_2$, 120; $MgCl_2$, 2; MgATP, 2; HEPES, 10; $CaCl_2$, 5; and ethylene glycol tetraacetic acid, 10 (pH 7.25 with CsOH); these solutions were made according to previous reports.[5,15]

Electrophysiology

Reconstituted calcium channel currents were recorded 36–48 h after transfection using the whole-cell patch-clamp technique at 38°C. After the baseline current was recorded, 1 μM nisoldipine was used to block the current. Reconstituted L-type calcium currents were obtained by digital subtraction of the two current traces.

The current–voltage curve was fitted with Boltzmann equation:

$$f(v) = I_{max} \times \frac{(V - V_{rev})}{\{1 + \exp[(V_h - v)/k]\}}$$

where I_{max} is the maximum current density, V is the activation voltage, V_{rev} is the reversal potential, V_h is the activation midpoint voltage, and k is the slope of the activation curve.

To obtain the inactivation time constant, time courses of inactivating current at 0, +10, and +20 mV were fitted to a single exponential function:

$$I_{Ca} = A\left[1 - \exp\left(\frac{-t}{\tau}\right)\right]$$

where I_{Ca} is the calcium current at time t (ms), A is the current amplitude, and τ (ms) is the inactivation decay time constant.

Statistical analysis

Continuous clinical data are expressed as mean ± standard deviation, and continuous patch-clamp data are expressed as mean ±

standard error (mean ± SEM). Differences between the two groups were examined using independent Student's *t*-tests. A *P* value <0.05 was considered statistically significant.

Results

Identification of mutations

We identified five novel *CACNA1C* variants in seven LQTS probands (2.5%): P381S, M456I, A582D, R858H (in three probands), and G1783C (*Figure 1*). These variants were absent in 500 reference alleles obtained from 250 healthy Japanese individuals and have not been previously reported according to the NHLBI Exome Sequencing Project Exome Variant Server (http://evs.gs.washington.edu/EVS). To achieve differentiation of rare variants identified in the healthy Japanese controls, we checked *CACNA1C* in 200 healthy Japanese subjects. There was only one non-synonymous variant (R1895Q), which was not reported in any SNP database (1/200 = 0.5%). An array of amino acid sequences among different species is shown below each electropherogram, indicating that every mutated amino acid is highly conserved (*Figure 1*).

Table 1 summarizes the clinical data of these probands. The mean QT interval was 468 ± 71 ms, and the mean QTc interval was 474 ± 58 ms. The mean HR was 63 ± 12 b.p.m., and the mean QRS interval was 76 ± 23 ms. Mean Schwartz score was 3.9 ± 1.2 points, and four of seven carriers had ≥3.5 points.

Clinical and genetic characteristics of seven proband families

Figure 2 summarizes the family trees of probands, and *Figure 3* shows their ECGs.

Family 1

A heterozygous p. P381S (c.1141 c>t) was identified in an asymptomatic 8-year-old girl (*Figure 1A*, II-3 in *Figure 2A*). Her 12-lead ECG revealed QT prolongation (*Figure 3A*). In an exercise stress test, her QTc interval prolonged to 548 ms at 3 min after exercise (see Supplementary material online, *Figure S1A*). Her father (I-2 in *Figure 2A*) and paternal half-sister (II-1 in *Figure 2A*) carried the same mutation and displayed QT prolongation (see Supplementary material online, *Figure S2A and B*). Her paternal half-sister (II-1 in *Figure 2A*) often experienced syncope while running and naturally

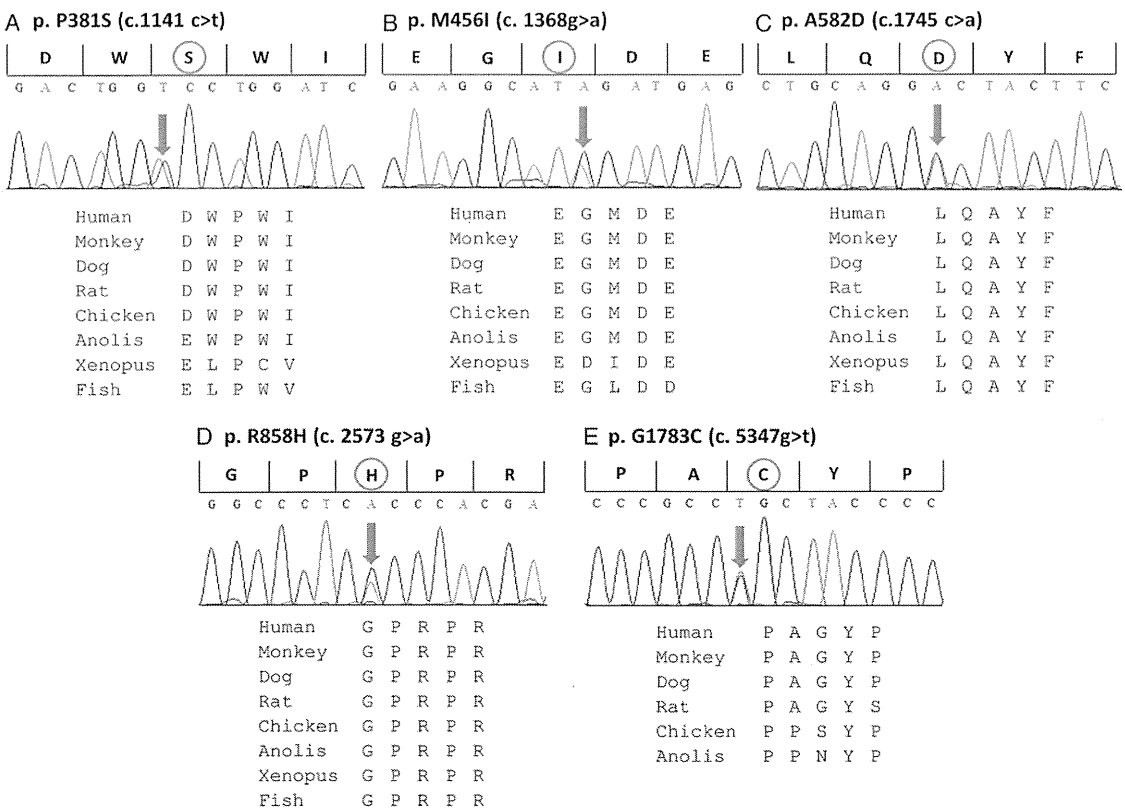

Figure 1 Identified mutations in *CACNA1C*. Upper: Electropherograms of mutant *CACNA1C* gene revealing heterozygous transitions. Lower: Amino acid sequence alignments. The amino acids are highly conserved among multiple species.

Table 1 Summary of *CACNA1C* mutations and mutation carriers

Patient	Age/ sex	Schwartz Score	Symptom	Family history of SD	HR (b.p.m.)	PR interval (ms)	QRS interval (ms)	QT interval (ms)	QTc interval (ms)	Mutation	Location
1	8/F	5	(−)	(−)	71	160	80	440	480	p.P381S	DIS6
2	12/F	3	(−)	(−)	73	180	60	420	464	p.M456I	DI/DII
3	12/F	5.5	(−)	(−)	56	140	60	620	597	p.A582D	DII S2/S3
4	54/F	4.5	VF	(+)	58	180	120	444	435	p.R858H	DII/DIII
5	7/M	2.5	(−)	(+)	77	160	60	420	476	p.R858H	DII/DIII
6	15/M	2.5	syncope	(−)	44	170	90	490	420	p.R858H	DII/DIII
7	58/F	4.5	syncope	(+)	63	140	60	440	449	p.G1783C	C-terminus

M, male; F, female; VF, ventricular fibrillation; SD, sudden death; HR, heart rate; QTc, corrected QT; D, domain; S, segment.

recovered, although it was uncertain that the syncope was due to ventricular arrhythmias.

Family 2

An asymptomatic 12-year-old girl showed heterozygous p. M456I (c.1368 g > a) (*Figure 1B*, II-1 in *Figure 2B*). Although her QTc interval showed mild prolongation at rest (486 ms) (*Figure 3B*), the interval prolonged to 568 ms at 3 min after exercise (stress test) (see Supplementary material online, *Figure S1B*). Her mother (I-2 in *Figure 2B*) was negative for this mutation, and her father's genomic DNA was not available.

Family 3

The third mutation was heterozygous p. A582D (c.1745 c>a) (*Figure 1C*), identified in a 12-year-old girl (II-2 in *Figure 2C*). Her QTc interval was significantly prolonged and notched in V4 (*Figure 3C*), and she had bradycardia (HR, 50 b.p.m.). The mutation was inherited from her mother (I-2 in *Figure 2C*), whose resting ECG also showed QT prolongation (612 ms) (see Supplementary material online, *Figure S2C*). The mother had paroxysmal atrial fibrillations and miscarried with her third child in 12 weeks of pregnancy because of prenatal cardiac arrest.

Family 4

One of three heterozygous p. R858H (c. 2339 g>a) carriers was a 54-year-old woman (*Figure 1D*, II-2 in *Figure 2D*). The proband was the third case in our previous report.[8] She had been successfully resuscitated during an electrical storm at midnight. Her father suddenly died at midnight at the age of 46, but no further information regarding him was available. The proband had been diagnosed with idiopathic VF. Her resting ECG displayed a bizarre complete right bundle-branch block (*Figure 3D*). After exercise, her QTc interval was prolonged to 567 ms with a 3 min recovery (see Supplementary material online, *Figure S1C*). She received an implantable cardioverter-defibrillator. At the first time, she was suspected as Brugada syndrome, and prescribed oral cilostazol (200 mg per day) to prevent VF; cilostazol is a phosphodiesterase inhibitor, which is related to the increase in HR and/or to an increase of calcium current.[16] However, cilostazol significantly increased her cardiac arrhythmic attacks. The subsequent replacement with a beta-blocker, atenolol (37.5 mg), completely prevented her VF. The same mutation was identified in her two daughters (III-1 and III-2 in *Figure 2D*). The elder daughter's ECG revealed QTc prolongation (QTc, 480 ms), but the younger's QTc interval was borderline (QTc, 444 ms) (see Supplementary material online, *Figure S2D and E*).

Family 5

The next heterozygous p. R858H carrier was a 7-year-old asymptomatic boy (not shown in *Figures 1* and *2*). He was noted to have QT prolongation at the regular health check-up at school (*Figure 3E*). His maternal uncle suddenly died during exercise at the age of 23. Other information and genomic DNA of his relatives were not available because they declined further medical examination.

Family 6

The last heterozygous R858H carrier was a 15-year-old boy (not shown in *Figures 1* and *2*). He was found unconscious on his way to